

The change in the microstructure of Hi-B electrical steel after normalizing

ZHAOYANG CHENG^a, JING LIU^{a,*}, JIAXIN YANG^b, WENSI CHEN^a, JIACHEN ZHU^a

^aThe State Key Laboratory of Refractories and Metallurgy, Wuhan University of Science and Technology, Wuhan, P.R. China, 430081

^bResearch & Development Center of WISCO, Wuhan, P.R. China, 430080

Hi-B electrical steel is a kind of soft magnetic materials with excellent magnetic properties. Normalization, as an important process, has great effect on final magnetic properties. The change in microstructure of Hi-B electrical steel was investigated in this paper. Optical microscopy, X-Ray diffraction (XRD) and transmission electron microscopy (TEM) are used to analyze the microstructure. It is found that the microstructure become more homogenous with more recrystallization grains after normalizing treatment. The texture intensity is increased after normalization treatment, especially the γ texture. Simultaneously, large numbers of small and dispersed AlN precipitate after normalizing treatment. The magnetic properties of the normalized specimen are much better than those of the not normalized specimen.

(Received November 21, 2013; accepted September 11, 2014)

Keywords: Hi-B electrical steel, Microstructure, Texture, Inhibitor, Normalization

The grain-oriented silicon steels are a type of soft magnetic materials mainly used for making the core in electrical transformers [1,2]. The grain orientation in this type of steels is characterized by the sharpness of $\{110\}\langle 001\rangle$ texture, i.e., Goss texture. As the inductance value B_8 is larger than 1.88T, the grain-oriented silicon steels are called Hi-B electrical steels [3]. The process to prepare it is complex, and has great influence on the final properties. Due to the extensive application and significant industrial value, the Hi-B electrical steels have attracted a lot of interests.

In recent years, a great deal of work has been done on the inhibitors and manufacture process of Hi-B electrical steels [4~6]. At present, the prevailing process for manufacturing the Hi-B electrical steels is the one stage cold rolling and the precipitates of AlN and MnS are used as co-inhibitors [7,8]. As the temperature for dissolving MnS is high, a high enough temperature must be used to dissolve the coarse MnS precipitate in a reasonably short length of time during the normalization stage, which is a preliminary heat treatment process after hot rolling but prior to cold-rolling. It has been found that the normalizing process plays an important role in determining the magnetic properties of the final products [9-11].

The normalizing process has great influence on the final properties of the Hi-B electrical steels. The change in the microstructure and in the characteristics of the inhibitor precipitates in the Hi-B electrical steels after normalizing was researched in this paper.

1. Experimental

The studied Hi-B electrical steels were refined and cast into ingot in vacuum induction melt furnaces at 1580~1600°C. The chemical composition of the studied Hi-B electrical steel was tested by chemical analysis method, and the result is shown in Table 1. The inhibitors in the steel were AlN and MnS. The steel was refined and cast into ingot in a vacuum induction melt furnace. The as-cast ingot was forged into the size of about 350×120×35 mm. It was then heated at 1250°C for 30 min, and subsequently hot rolled to a thickness of 2.3mm through 5 passes. In order to obtain dispersed and small inhibitor precipitates (MnS and AlN), steps were taken to ensure that the temperature of the steel before entering the hot rolling roller was above 1190°C and the final rolling temperature was above 950°C. The hot rolled sheet was normalized at 1120°C for 3 min.

Specimens were polished and etched with a solution of 4% nitric acid in alcohol at room temperature. Optical microscopy was utilized to observe the microstructure of the specimens. Texture was measured by X-ray diffraction (XRD, D/MAX-2500PC) with Mo $K\alpha$ radiation. The inhibitor precipitates were analyzed by transmission electron microscopy (TEM) JEM-2100F, and the composition of the inhibitors were analyzed by energy dispersive X-ray spectroscopy (EDS). The magnetic properties were measured on the AC/DC magnetic measuring instrument (MPG-100D) using the sheets with a size of 30mm×300mm.

Table 1. Chemical composition of Hi-B electrical steels (wt%).

Si	C	Mn	Cu	Als	S	N	Fe
3.16	0.042	0.08	0.4	0.014	0.02	0.0082	Balance

2. Results and discussion

2.1. Metallographic microstructure

The metallographic microstructure of the hot-rolled and normalized specimens with different magnifications is shown in Fig. 1. Fig. 1 (a), (b), (c) and (d) are lower magnification micrographs and (a'), (b'), (c') and (d') are the respective higher magnification micrographs. It is seen from the lower magnification micrographs that the microstructure is quite inhomogeneous along the direction of thickness. It can be divided into three areas: the surface decarburization layer, the secondary surface layer and the center area. The surface decarburization layer contains mainly the fine equiaxed ferrite grains, which are the source of the secondary recrystallization nucleus. The secondary surface layer contains equiaxed grains along with some recrystallization grains, which will promote the growth of the secondary recrystallization grains. The grains in the center are deformed ferrite grains, which inhibit the growth of the secondary recrystallization grains. These results correspond to those of other researchers [9]. As the sheets are very thin and the surface of the sheets contacts with the atmospheric environment, the surface becomes cool very fast and the temperature along the thickness direction is different. Meanwhile, the shear deformation during the rolling process is also quite different along the thickness direction. The inhomogeneous microstructure along the thickness direction is attributed to the temperature and the shear deformation difference along with the thickness direction during the hot rolling process. So it will produce the irregular distribution of elastic strain along the thickness direction. The recovery and recrystallization degree along the thickness direction is quite different in the wake of strain difference, and the surface of the specimen gives place to the recrystallization soon.

The microstructure of the normalized specimen is more homogeneous than the hot-rolled specimen to some extent (Figs. 1a' to 1d'). There are some fine and equiaxed recrystallization grains in normalized specimen, especially in the intersecting surface. However, the normalizing time is too short to allow full recovery and recrystallization.

The grain size of the specimens is calculated on the basis of the EBSD analysis. The average grain size of the hot rolled specimen is 10.84 μm , while that for the normalized specimen is 12.71 μm . So difference in grain size between the hot rolled and normalized specimens is small, which can also be seen clearly from the micrographs (Fig. 1).

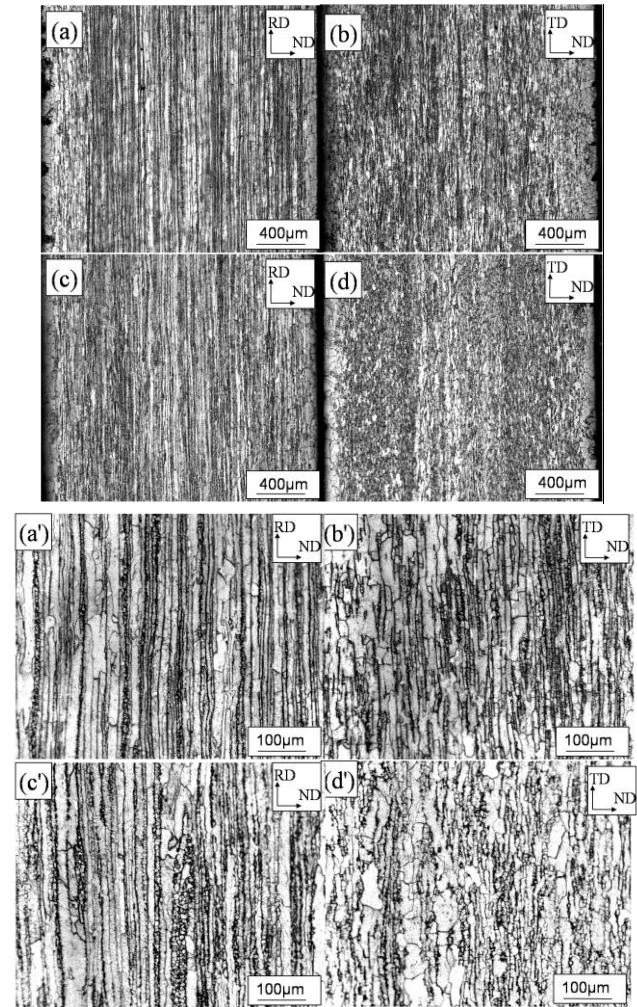


Fig. 1. Metallographic Microstructure of the specimens: (a),(a') and (b), (b'): hot-rolled specimen (c), (c') and (d), (d'): normalized specimen.

Based on the metallographic analysis, it can be suggested that the microstructure becomes more homogeneous and the number of recrystallization grains is increased after normalizing treatment.

2.2. Texture

The Orientation Distribution Function (ODF) sections of the surface of the specimens are given in Fig. 2 and Fig. 3. There is very little texture in the hot-rolled specimen (Fig. 2), in which the main component of the texture is $\{112\}\langle 111 \rangle$ (Φ is around 35°). Much more texture is present in the normalized specimen (Fig. 3) and the intensity of the texture is stronger than that in the hot-rolled specimen. The main components of the texture in the normalized specimen are $\{112\}\langle 111 \rangle$ (Φ is around 35°), $\{110\}\langle 557 \rangle$ (Φ is around 90°) and $\{111\}\langle 112 \rangle$ (Φ is around 55°). The intensity of all of this texture increases after normalizing treatment. However, the increase in the intensity of the $\{110\}\langle 557 \rangle$ and $\{111\}\langle 112 \rangle$ texture is

larger than the increase in the intensity of the $\{112\}\langle 111 \rangle$ texture. S. K. Chang [10] found that the $\{111\}\langle 112 \rangle$ texture will form high-angle boundaries with $(110)[001]$ (GOSS texture). The GOSS texture will grow up through the migration and expanding of the high-angle boundaries, simultaneously, the $\{111\}\langle 112 \rangle$ texture will be annexed. Therefore, the increased texture, i.e. $\{110\}\langle 557 \rangle$ and $\{111\}\langle 112 \rangle$ texture, is a favorable microstructure for the subsequent secondary recrystallization annealing treatment aimed to optimize the final magnetic properties in grain oriented silicon steels.

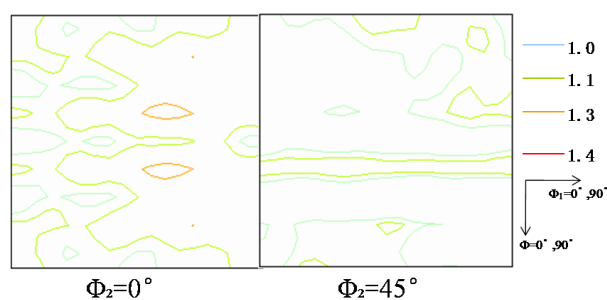


Fig. 2. Orientation Distribution Function (ODF) of the hot-rolled.

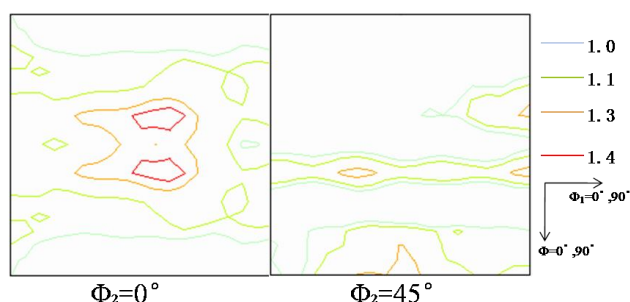


Fig. 3. Orientation Distribution Function (ODF) of the normalized specimen.

2.3. Inhibitors

The morphology and EDS spectra of the inhibitors in the specimens are shown in Fig. 4 and Fig. 5. There are many precipitated phases in the hot rolled specimen, which are either spherical or irregular in shape (Fig. 4) and distributed mostly in grain boundaries. According to the EDS spectra, the main inhibitors of the hot-rolled specimen are MnS, CuS and $(\text{Mn,Cu})\text{S}_x$, with a small amount of AlN. MnS inhibitor is with quite large size, while CuS is with very small size. There still are some other kinds of inhibitors, just like that $(\text{Mn,Cu})\text{S}_x$ compound and AlN. The size of the $(\text{Mn,Cu})\text{S}_x$ compound is larger than CuS, while smaller than MnS. The small amount of AlN is coarse block. According to the different in the inhibitor type, the AlN inhibitor is divided into three kinds conventionally, i.e. A, B, C types, which with the

type of fine needle, fine disk, coarse block, respectively [12]. So a small number of C type AlN inhibitor precipitate during the hot rolling process. This result agrees with the research of YANG Jia-xin et al [13], who found that the inhibitors precipitated in the Hi-B electrical steels during the hot rolling process were mainly MnS, CuS, $(\text{Mn,Cu})\text{S}_x$ and a small number of AlN.

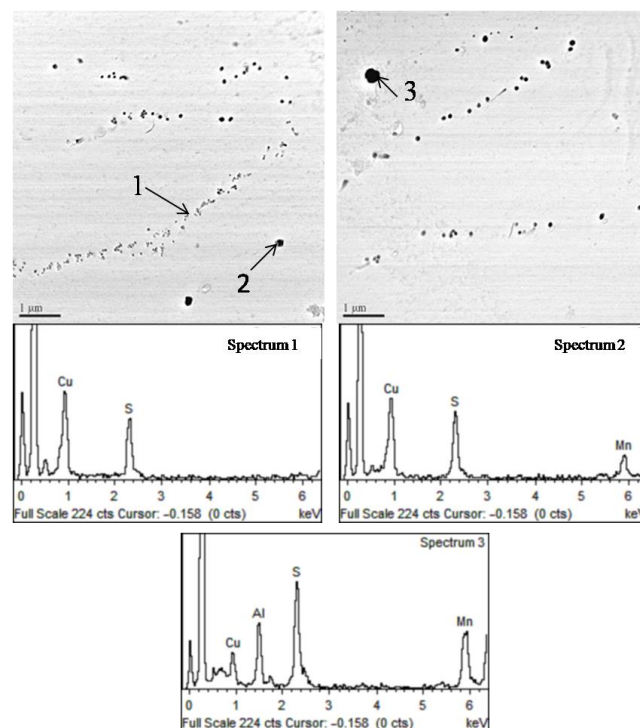


Fig. 4. Morphology of precipitated phases and corresponding component analysis in the hot-rolled specimen.

Large number of precipitates are presented and distributed homogeneously in the normalized specimen (Fig. 5), most of which are irregular in shape. According to the EDS spectra, the main inhibitors of the normalized specimen are AlN, with a small amount of MnS, CuS and $(\text{Mn,Cu})\text{S}_x$. The type of MnS, CuS and $(\text{Mn,Cu})\text{S}_x$ inhibitors maintains from the hot-rolled specimen to the normalized specimen almost without growth during the normalizing treatment. There are two kinds of AlN inhibitors in the normalized specimen, i.e. B type and C type. The C type AlN inhibitor maintains the type of hot-rolled specimen. Large numbers of the fine disk, i.e. B type, AlN inhibitor precipitates homogeneously from the matrix during the normalizing treatment. T. Sakai et al [12] also found that large numbers of the B type AlN inhibitor precipitated homogeneously during the normalizing treatment.

From the above, we can make a brief conclusion that the main inhibitors of the hot-rolled specimen are coarse MnS and fine CuS, while the main inhibitor of the normalized specimen is B type AlN. The AlN inhibitor

with the type of fine disk precipitates equally during the normalizing treatment. The MnS and CuS inhibitors have no change during the normalizing treatment.

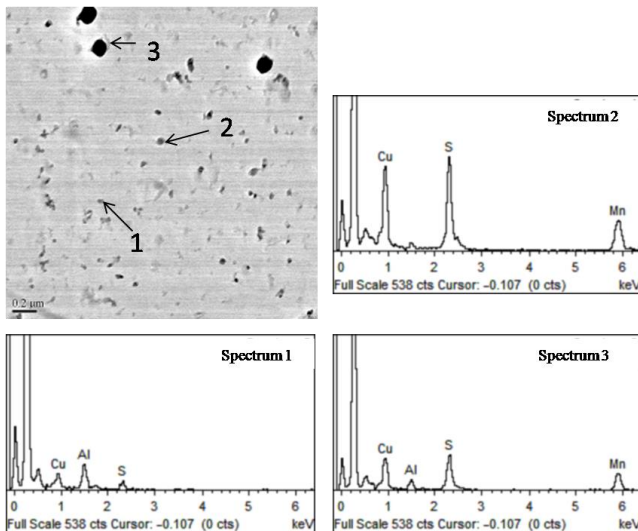


Fig. 5. Morphology of precipitated phases and corresponding component analysis in the normalized specimen.

2.4. Magnetic properties

The magnetic properties of the two specimens with the same cold rolling and heat treatment process are given in Table 2. The magnetic properties of the normalized specimen are much better than the not normalized specimen. The iron loss value $P_{1.7/50}$ of the normalized specimen is 1.173 W/kg, much lower than that of the not normalized specimen (2.766 W/kg). The inductance value B_8 of the normalized specimen is 1.892 T, which is much higher than that of the not normalized specimen (1.426 T). These results suggest that the normalizing treatment plays an important role in the excellent magnetic properties of the Hi-B electrical steel.

Table 2. Magnetic properties of the experimental specimens.

Specimens	$P_{1.7/50}$ (W/kg)	B_{800} (T)
Not normalized	2.766	1.426
Normalized	1.173	1.892

3. Conclusions

The microstructure becomes more homogeneous and the number of recrystallized grains is increased after the normalizing treatment. Simultaneously, the texture intensity is increased after the normalizing treatment, especially the γ texture, which will promote the preferred growing of GOSS texture. Finally, a large number of small and dispersed AlN (B type) inhibitor particles precipitate during the normalizing process, which will effectively hinder the growth of the primary recrystallization grains and promote the growing of GOSS texture. The magnetic properties of the normalized specimen are much better than those of the not normalized specimen.

Acknowledgement

This work is supported by the National Basic Research Program (863 Program) of China (Grant No.2012AA03A506) and the Provincial Natural Science Foundation of Hubei, China (Grant No. 2008CDA040).

References

- [1] C. Gheorghies, A. Doniga, Journal of Iron and Steel Research, International, **16**(4), 78 (2009).
- [2] N. A. Castro, M. F. De Campos, F. J. G. Landgraf, Journal of Magnetism Magnetic Materials, **304**, 617 (2003).
- [3] J. Iwanaga, H. Masui, J. Harase, et al. Materials Engineering and Performance, **3**(2), 223 (1994).
- [4] Y. Ushigami, T. Kumano, T. Haratani, et al. Materials Science Forum, **853**, 467 (2004).
- [5] Y. Hayakawa, J. A. Szpunar, Acta materialia, **45**(3), 1285 (1997).
- [6] Lihua Liu, Lijuan Li, Junjun Huang, et al. Journal of Magnetism Magnetic Materials, **324**, 2301 (2012).
- [7] Lu Feng-xi, Yao Cheng-jun, Metallic Functional Materials, **13**(3), 34 (2006).
- [8] Lu Feng-xi, Yao Cheng-jun, Metallic Functional Materials, **13**(4), 36 (2006).
- [9] Yoshihiro Ozaxi, Mineo Muraki, Takashi Obara, ISIJ International., **38**(6), 531 (1998).
- [10] S. K. Chang, Materials Science and Engineering A, **452-453**, 93 (2007).
- [11] Zhaosuo Xia, Yonglin Kang, Quanli Wang. Journal of Magnetism and Magnetic Materials, **320**, 3229 (2008).
- [12] Sakai Tomohiko, Shimazu Takahide, Chikuma Kentarou, et al. ISIJ, **70**(15), 2049 (1984).
- [13] Yang Jia-xin, Liu Jing, WISCO Technology, **45**(5), 38 (2007).